Bull. Mater. Sci., Vol. 37, No. 2, April 2014, pp. 213–219. © Indian Academy of Sciences.

One-pot synthesis of hydroxyapatite–silica nanopowder composite for hardness enhancement of glass ionomer cement (GIC)

ISMAIL AB RAHMAN*, SAM'AN MALIK MASUDI, NORHAYATI LUDDIN and RAYEES AHMAD SHIEKH

School of Dental Sciences, Universiti Sains Malaysia, 16150 Kubang Kerian, Kelantan, Malaysia

MS received 28 June 2012; revised 17 January 2013

Abstract. **Hydroxyapatite–silica nanopowder composite was prepared using one-pot sol–gel technique. The morphology of the powder consists of a mixture of spherical silica particles (∼30 nm) embedded within the elongated hydroxyapatite (∼103 nm). The synthesized nanoparticles were incorporated into commercial glass ionomer cement (GIC) and Vickers hardness was evaluated. Results shown that the addition of the nanopowder composite gave ∼73% increment in the hardness compared to the pure GIC. Higher content of hydroxyapatite–silica nanopowder resulted in dense cement and produced a stronger GIC and the application of this material with improved hardness property might lead to extend the clinical indications, especially in stress bearing areas.**

Keywords. **Hydroxyapatite–silica nanopowder; sol–gel technique; glass ionomer cement; hardness.**

1. Introduction

Glass ionomer cements (GICs) are water-based cements, have been widely used as restorative dental-filling materials. The materials are based on the reaction between an alumino–silicate glass and polyacrylic acid and the cements are formed via acid–base reactions between the components (McLean and Gasser 1985). The matrix of the set cement is an inorganic–organic network with a highly cross-linked structure. The application of GICs as restorative dental materials is mainly due to the biocompatible property that able to form direct bonding to the tooth structure and the release of fluoride ions that protect against dental caries (Walls 1986; Xie *et al* 2000). However, GICs are brittle and have poor mechanical properties that include low fracture strength, fracture toughness and wear resistance. These properties are their main disadvantages that limit their extensive use in dentistry as a filling material in stress-bearing application (Lohbauer 2010).

A number of efforts to improve the mechanical properties of GICs have been made in several aspects. These include the incorporation of a reinforcing phase such as metal particles or alumina, zirconia or glass fibres (Kerby and Bleiholder 1991; Lohbauer *et al* 2004; Gu *et al* 2005; Yli-Urpo *et al* 2005). However, the improvement on mechanical properties was not significant. In all cases, commercial powders with particle size in micro range were used. In recent years, hydroxyapatite ($Ca_{10}(PO_4)_6(OH)_2$, HA) has shown promising advantages in restorative dentistry, including its biocompatibility, hardness similar to that of natural tooth and intrinsic radiopaque response (Arcis *et al* 2002; Arita *et al* 2003; Wang and Shaw 2009). Although, it is a naturally occurring mineral form of calcium apatite, technological advances have enabled nanosized HA to be prepared by many different methodologies, for instances, wet-chemical preparation, sol–gel synthesis and co-precipitation, etc (Dorozhkin 2010). The ability of HA to integrate with bone structure can help bonding between bone and implant structures and also support bone growth (Nicholson *et al* 1993; Moshaverinia *et al* 2008). Therefore, the incorporation of HA into GIC may not only improve the biocompatibility of GICs but also have the potential of enhancing the mechanical properties. A number of researchers have attempted to evaluate the effect of the addition of HA powders into GICs on mechanical properties. Until now, effect of addition of HA on the compressive strength, diametral tensile strength (Moshaverinia *et al* 2008), flexural strength (Arita *et al* 2003), toughness, bonding and fluoride-release properties (Lucas *et al* 2003) of GICs have been reported. However, incorporation of HA–silica nanopowder composite prepared by one-pot technique into GICs is not yet reported. Thus, this study is aimed to synthesize HA–silica nanocomposites by one-pot sol–gel technique and to assess the effect of their addition on the hardness of GICs. It is envisaged that the nanosilica particles may fill the void between HA particles, subsequently enhance the packing density and further improve the hardness of GICs.

*Author for correspondence (arismail@usm.my)

2. Experimental

2.1 *Synthesis of nanosilica*

Nanosilica was prepared using sol–gel method as described by Jafarzadeh *et al* (2009). A mixture of absolute ethanol (99·5%, Systerm), tetraethoxysilane (TEOS, 99%, Fluka) and distilled water in a volume ratio of 30:5:1 was mixed under low frequency ultrasound (Bransonic, Model 5510, 42 kHz) at room temperature. Ammonia was added into the mixture at a controlled fed rate. The gel formed was centrifuged and washed with ethanol and distilled water. Drying was carried out for overnight in a freeze dryer (Labconco, Freezon 12), followed by calcination at 600 °C for 1 h.

2.2 *Synthesis of hydroxyapatite*

Nanohydroxyapatite was produced by using sol–gel method (Panda *et al* 2003). Calcium hydroxide (>98%, RM Chemicals) and phosphoric acid (>99%, Aldrich) were the sources of calcium and phosphorus. Initially, 7·408 g of calcium hydroxide was mixed into 100 ml of distilled water in a glass beaker and stirred for 30 min using a magnetic stirrer, until all calcium hydroxide powder was well mixed to form suspension. After that, 4·104 ml of phosphoric acid was added drop wise to the suspension. The pH of the suspension was adjusted to the range of 11–12 using ammonia. The suspension was stirred for 48 h to obtain a white viscous sol. The sol was filtered, freeze dried and calcined at 600 °C for 1 h.

2.3 *One-pot synthesis of hydroxyapatite–silica–nanocomposite*

The flowchart shown in figure 1 outlines the experimental procedure used to synthesize the hydroxyl–silica–nanocomposite in this study.

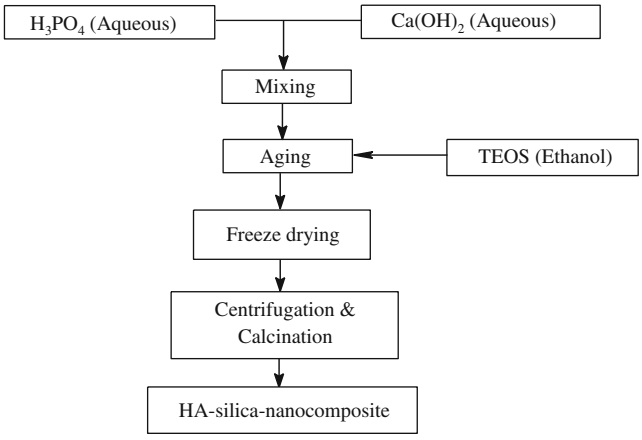

Figure 1. A flow chart of one-pot sol–gel synthesis of HA–silica–nanocomposite.

First, the nanohydroxyapatite (HA) was prepared by the procedure in § 2.2. A quantity of 5 ml of TEOS that had dissolved in 10 ml of ethanol was added drop wise into the sol for 12 h. The sol was centrifuged, dried using a freeze dryer and calcined at 600 °C for 1 h. The same procedure was repeated for addition of 10 and 20 ml TEOS.

Based on the following chemical equations, the theoretical composition of silica and HA in the composites were calculated.

$$5Ca(OH)_2 + 3H_3PO_4 \rightarrow Ca_5(PO_4)_3OH + 9H_2O,$$

$$Si(OC_2H_5)_4 + 2H_2O \rightarrow SiO_2 + 4C_2H_5OH.$$

Table 1 shows the percentage of silica in each 5, 10, 20 ml addition of TEOS were found to be 11, 21, 35%, respectively. Thus, the samples were labelled as HA–11SiO_2, HA–21SiO_2 and HA–35SiO_2.

2.4 *Preparation of nano–HA–silica–added GIC*

A commercial GIC (Fuji IX GP, GC International Japan) was used as the control and base material. HA, HA–11SiO_2, HA–21SiO_2, HA–35SiO_2 and silica were mixed into GIC at various percentages (by weight): 1, 3, 5, 7, 9, 15 and 20%, respectively. Each powder mixture was gently ground manually for 10 min using pestle and mortar. The cements were made by spatulation of the powder mixture into the liquid at a powder/liquid ratio of 1:1 and mixed according to the manufacturer's instructions.

The cement was then inserted into a mold with internal perforation dimension of 5·0 mm diameter and 2·0 mm height. The mold was positioned on a glass slide with a celluloid strip interposed. The cement was introduced into the mold by plugger and the upper surface was covered with another celluloid strip. A second glass slide was compressed on the upper surface of the mold in order to obtain specimens with flat surfaces (Magni *et al* 2010). Cements were covered with moisten gauze after completion of initial reaction and left undisturbed for 24 h to enable complete setting reaction.

2.5 *Hardness measurement*

Vickers hardness measurements were taken at 24 h after the initial setting reaction (Fuel Inst. Ltd). The surface of the cement was first polished using 1000 grit silicon carbide paper. The load applied on the sample was 5 kg and the indentation was applied for 15 s. Only one diamond indentation was made on top of each specimen's surface and measurement was taken. The measurements were triplicate for each percentage of materials. The mean of these measurements were then converted into Vickers hardness values.

2.6 *Characterization and data analysis*

Morphology of the samples was examined using transmission electron microscopy (TEM, Philips CM12) and

Table 1. Powder composition of different composites.

Composite	Mass of HA (g)	Mass of silica (SiO_2) (g)	Powder composition
HA + 5 ml TEOS	10·04	1·356	89%HA, 11% SiO_2
HA + 10 ml TEOS	10·04	2·712	79%HA, 21%SiO_2
HA + 20 ml TEOS	10·04	5·423	65%HA, 35%SiO_2

scanning electron microscopy (SEM, Leo Supra 50 VP). Data were analysed using descriptive statistics under the package of SPSS version 16.0. Fourier transform infrared spectra were recorded using a Perkin–Elmer 2000 FTIR spectrometer in the frequency range of 400–4000 cm^{-1}.

3. Results and discussion

3.1 *Characterization of nanopowders*

Morphologies of nanosilica and nonohydroxyapatite powders were prepared by sol–gel technique, as observed under TEM are shown in figure 2. The images verified the elongated shaped are indeed HA and the spherical powders are silica (Panda *et al* 2003; Jafarzadeh *et al* 2009). These images revealed that all the powders are in nanosize range with the mean size of the elongated HA ∼103 nm and silica ∼30 nm. The morphology of the hydroxyapaite–silica powder nanocomposite consists of a mixture of spherical silica particles embedded within the elongated hydroxyapatite (figure 3). The microstructure for the composite system under dot mapping SEM shows clearly the distribution of various components, packing density of different particle size of fillers within matrix of GIC, such as silica and phosphorus (figure 4).

Figure 5 shows FTIR spectra of the samples comparing the functional groups present in silica (a), silica–hydroxyapatite (b) and hydroxyapatite (c) after calcinations at 600 °C. FTIR analysis of the samples before and after calcinations suggests that the synthesized silica nanoparticles are pure and free of organic contaminants. Si–O–(H···H_2O) bending vibration observed at ∼960 cm^{-1} while peak at ∼804 cm^{-1} indicates in-plane bending vibrations of geminol groups. Peak at 1100 cm^{-1} indicates Si–O–Si asymmetric stretching vibrations; ∼3428 cm^{-1} denotes surface –OH groups while the bending of –OH groups (adsorbed water molecules) at ∼1635 cm^{-1} (Vasant *et al* 1995; Green *et al* 2003; Rahman *et al* 2007) (figure 5a).

The representative FTIR spectrum (c), showing all characteristic absorption peaks of pure or stoichiometric hydroxyapatite at ∼1000–1100 cm^{-1} (Varma and Babu 2005). The bands at 960–965 and 566–602 cm^{-1} correspond to n_1 and n_4 symmetric P–O stretching vibration of PO_4^{3-} ion, respectively (Kawata *et al* 2004; Miyaji *et al* 2005). As a major peak of phosphate group, n_3 vibration peak could be identified in the region between 1100 and 962 cm^{-1}, which

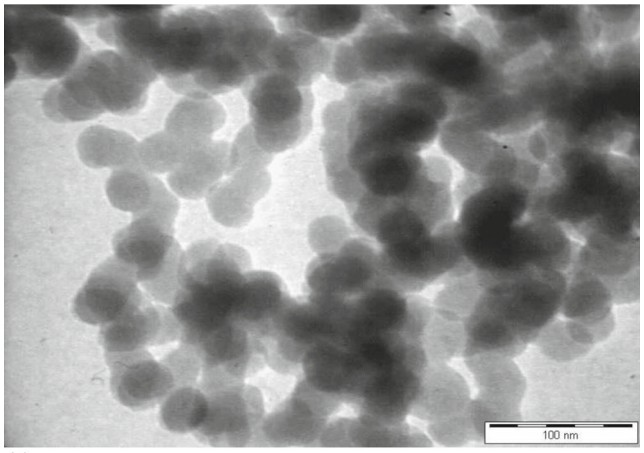

(a)

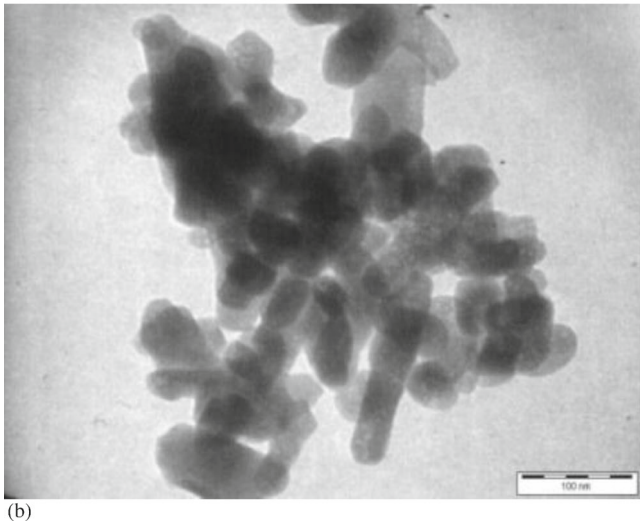

(b)

Figure 2. TEM of (**a**) nanosilica and (**b**) nanohydroxyapatite.

is the most intensified peak among the phosphate vibration modes. The bands between 566 and 602 cm^{-1} belong to n_4 vibration mode of phosphate group which occupies two sites in the crystal lattice at 602 and 566 cm^{-1}. Two distinguishable splitting of n_4 vibrations indicated the low site symmetry of molecules, as two peaks confirmed the presence of more than one distinction site for the phosphate group in hydroxyapatite lattice (Rehman and Bonfield 1997). The band assigned to the stretching mode of hydroxyl (OH) in the hydroxyapatite (3570, 640, 475 cm^{-1}) (Kawata *et al* 2004; Varma and Babu 2005; Rozita *et al* 2011) can be clearly observed in the spectra. Thus according to the observed

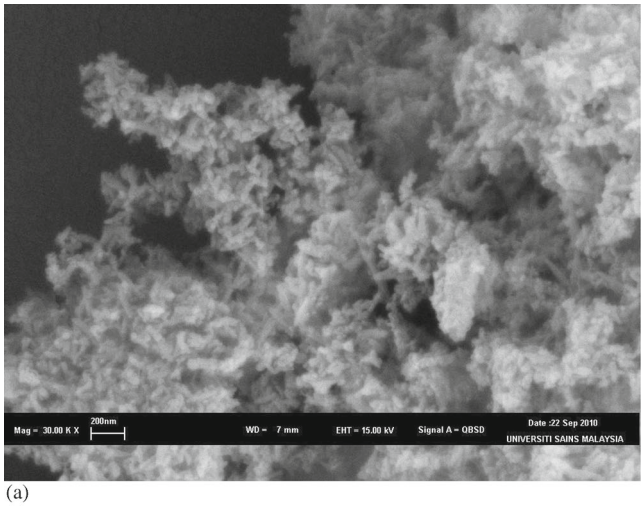

(a)

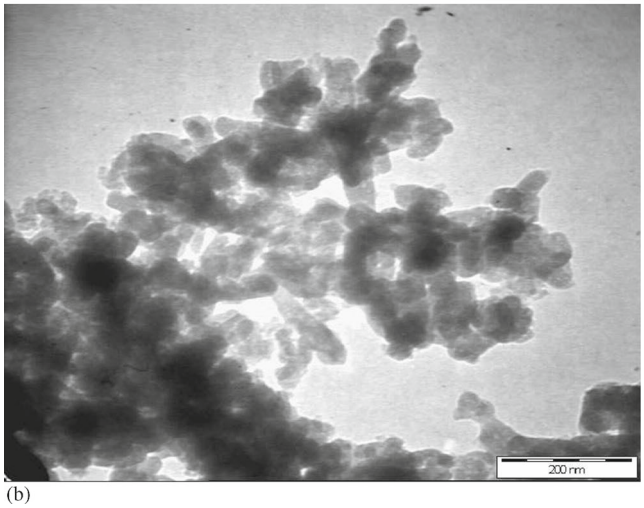

(b)

Figure 3. Micrographs of HA–11SiO_2 nanocomposite (**a**) SEM and (**b**) TEM.

stretching frequencies and the similarity of FTIR spectra of the investigated samples, the possible formation of hydroxyapatite–silica nanopowder composite by sol–gel technique could be suggested (figure 5b).

3.2 *Vickers hardness of HA–silica–GIC*

Hardness is one of the most important mechanical properties of a dental materials. It provides an indication of the resistance of the material for scratching or abrasion. Surface hardness tests appear to be appropriate for evaluating the degradation and durability of dental materials, to observe the effect of storage mediums on the surface, as indicative of resistance to wear and durability and also to monitor the hardening process of cements (Shintome *et al* 2009). A large hardness means greater resistance to plastic deformation or cracking in compression and contributes to better wear properties. In this study, the Vickers hardness of a new HA–silica–GIC nanocomposites was evaluated against a pure GIC.

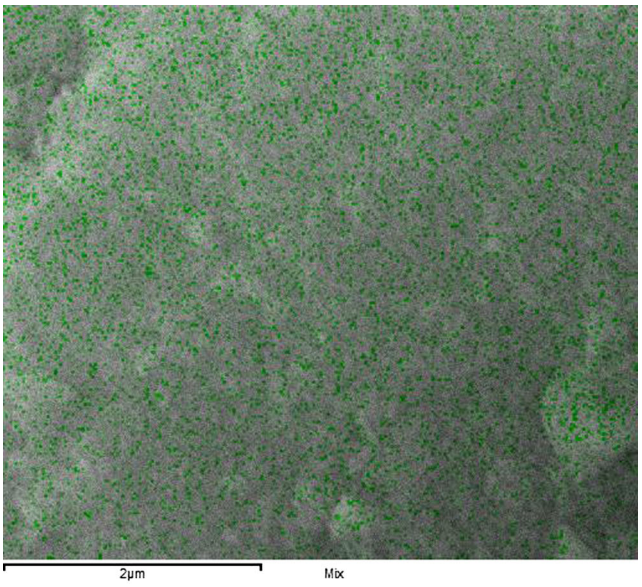

(a)

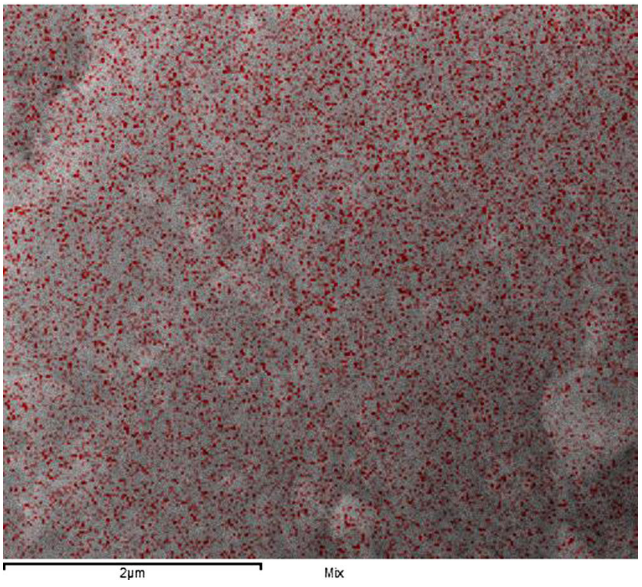

(b)

Figure 4. Distribution pattern of different particle size of fillers within the matrix of GIC, (**a**) silicon dot-maping and (**b**) phosphorus dot-mapping.

Based on literature, the works on the Vickers hardness of GIC is very limited. This is further complicated by the different loading force and dwelling time adopted by different researchers in their respective studies. Silva *et al* (2007) reported that the mean Vickers hardness of Fuji IX as 41·0HV (±4·03) with loading force of 100 g for 30 s while Yap *et al* (2002), using 5 kg load with a dwelling time of 15 s demonstrated Vickers hardness of GIC as 54·4HV (±7·88). The mean Vickers hardness of pure GIC (Fuji IX) used as control is 40·6HV (±6·95) by using the applied load of 5 kg for 15 s. Thus, the hardness of GIC

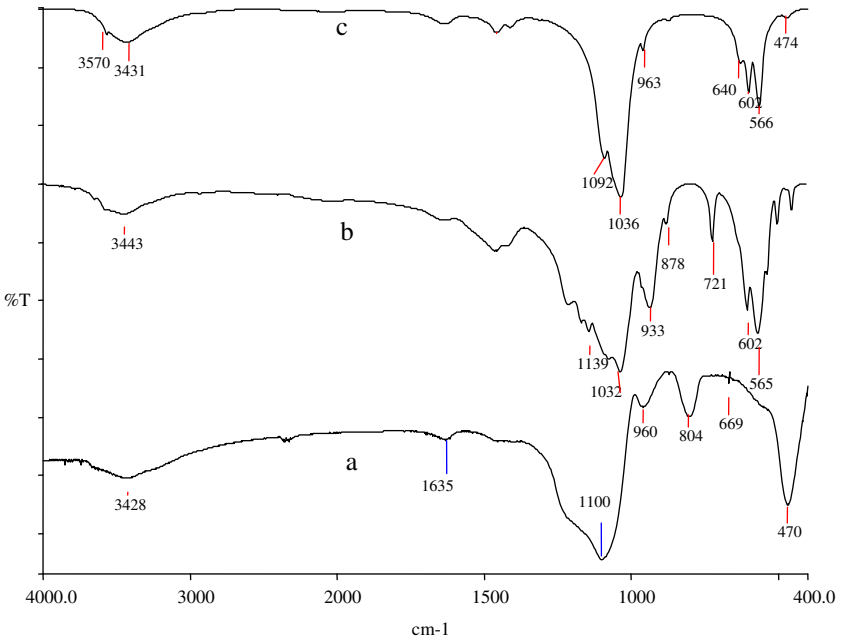

Figure 5. FTIR spectra of (**a**) silica, (**b**) HA–11silica and (**c**) HA.

measured in this study falls within the range of 40–55HV. Table 2 summarized the Vickers hardness mean values and standard deviations (SD) for each group of HA–silica–GIC at different percentage. The mean values are also represented graphically in figure 6 in order to compare the Vickers hardness of different groups of HA–silica–GIC with pure GIC.

Figure 6 reveals that all the HA–silica nanopowder-added GIC follow the same trend except for HA–35SiO_2–GIC. Generally, addition of 1% HA–silica nanocomposite, regardless of the composition of silica gives the highest hardness values. Further addition of HA–silica nanocomposite in a higher percentage resulted in a steady decrease of hardness, with the lowest hardness noted at 20% of HA–GIC (30·6HV), followed by 20% HA–11SiO_2–GIC (34·5HV) and 20% HA–21SiO_2–GIC (37·7HV). Hardness of 20% HA–35SiO_2–GIC (43·5HV) and 20% silica–GIC (48·2HV) also exhibited the lowest hardness among their respective group, however, their values are still higher than the pure GIC (40·6HV). HA–35SiO_2–GIC shows steady increase in hardness with further addition of the nanocomposite, reaching its peak at 5% HA–35SiO_2–GIC (70·8HV) that gives hardness enhancement of ∼73%. Nevertheless, further increase in HA–35SiO_2 content in GIC resulted in the decrease in hardness.

Referring to figure 6, HA–35SiO_2–GIC exhibits the best improvement of hardness among all the groups. As showed by TEM and SEM micrographs (figure 3), the synthesized HA–silica nanopowder composite comprised of larger HA with elongated and smaller spherical silica particles. It is believed that by mixing the different sizes and shapes of HA–silica nanoparticles into GIC apparently leading to higher packing density of the composite and thus greater resistance to surface indentation. The silica particles not only fill the void between the elongated shape of HA particles, but also occupy the empty spaces between the glass ionomer particles and act as a reinforcing material in the composition of GIC that enhanced the Vickers hardness. This phenomenon is schematically represented in figure 7. In addition, a homogeneous distribution of HA–silica nanoparticles in the composites is clearly shown in figure 4. However, the addition of HA–35SiO_2 saturates at 5% (others 1%), which lead to a decrease in hardness of the cement upon further addition. This may be due to the over-crowding of the fillers and reduction in interfacial bonding between the particles and ionomer matrix. The unreacted portion of the glass particles are sheathed by silica that develops during the removal of cations from the surface of the particles. Thus, the set cement contains an agglomeration of unreacted powder particles surrounded by silica in an amorphous matrix of hydrated calcium and aluminum polysalts.

Since no previous study on the incorporation of HA–silica nanopowder into GIC has been reported, this phenomenon can be compared with previous reported works on mechanical properties of GIC incorporated with microsize of HA. Experimental studies done by Yap *et al* (2002) using Fuji IX at a powder/liquid mass ratio of 0·362:0·10, revealed that the highest Vickers hardness was obtained with the use of 4% HA–GIC (68·17HV ± 3·72). Gu *et al* (2005) demonstrated that 4% HA/ZrO_2–GIC composition exhibited the highest Vickers hardness (67·42HV ± 2·74). On the other hand, Arita *et al* (2003) also used Fuji IX but at powder/liquid ratio of 1·75, reported that the highest flexural strength was obtained at 19% HA–GIC. Other researchers have attempted to incorporate reactive glass fibres (Lohbauer *et al* 2004),

Table 2. Mean and standard deviation (SD) of Vickers hardness for each group of HA–silica nanocomposite at different percentage.

	HA–GIC		HA–11SiO_2–GIC		HA–21SiO_2–GIC		HA–35SiO_2–GIC		Silica–GIC	
%	Mean	SD	Mean	SD	Mean	SD	Mean	SD	Mean	SD
1	55·1	9·75	64·5	3·02	67·5	5·67	61·1	3·15	66·4	6·88
3	54·1	4·80	54·7	5·54	65·1	1·31	67·7	8·88	53·1	4·62
5	47·3	6·03	51·8	1·19	54·6	3·16	70·8	11·20	52·9	6·82
7	41·0	6·58	45·4	2·55	52·8	1·53	60·1	12·14	53·5	7·56
9	32·0	8·78	42·9	6·08	50·4	4·19	52·6	4·83	49·8	6·11
15	32·9	7·28	40·9	2·66	46·6	2·09	43·9	5·88	47·9	10·43
20	30·6	5·75	34·5	1·15	37·7	1·04	43·5	4·09	48·2	8·47

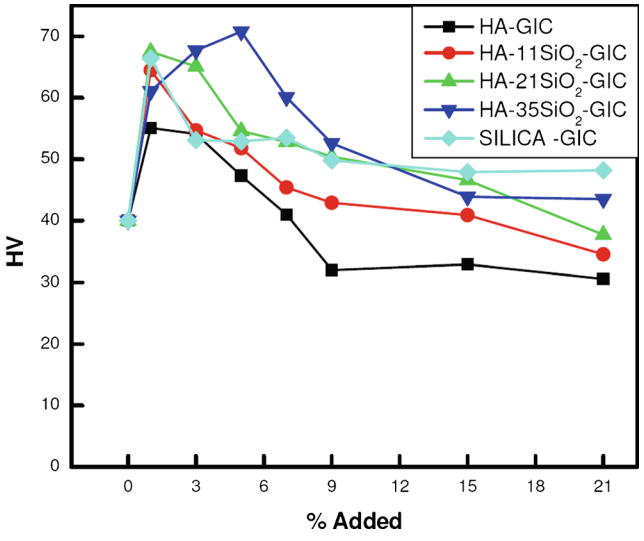

Figure 6. Comparison of Vickers hardness between different groups of HA–silica–GIC and conventional GIC.

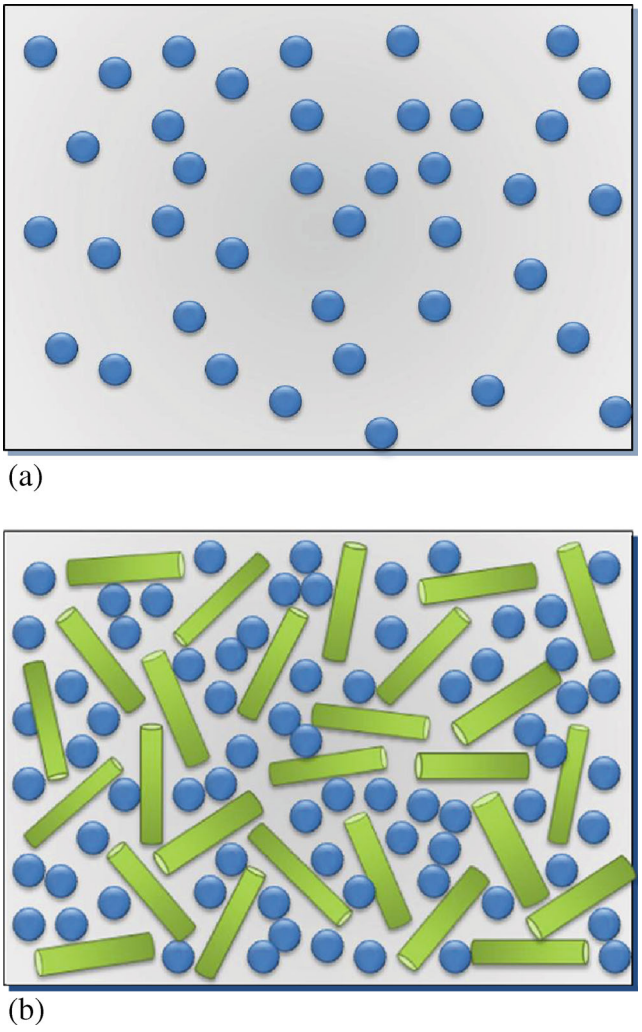

Figure 7. Schematic diagram of packing density of different particle size of fillers within the matrix of GIC (● = nanosilica, (▬ = elongated HA): (**a**) with silica nanoparticles and (**b**) with HA–silica nanoparticles.

bioactive glass (Yli-Urpo *et al* 2005) into GIC. Nicholson *et al* (1993) suggested that the incorporation of HA into GIC can only be achieved at low powder-to-liquid ratios, due to high bulk density of HA powder. In this study, Fuji IX was used and mixed at powder/liquid ratio of 1:1. HA and silica particles of nanosize were used instead of micro-size HA particles. It is apparent that powder/liquid ratio of the mixing cement, size of HA particles incorporated in relation with size of glass particles affect the resulted cement hardness. The relationship between them warrants further investigation.

It is interesting to compare the highest hardness value obtained from this study with other restorative materials. The hardness of 70·8HV (±11·20) achieved by adding 5% HA–35SiO_2–GIC is comparable with the hardness of commercial composite resins, Z250 (69·0HV ± 3·73), (Silva *et al* 2007) and Z100 (79·76HV ± 9·66), (Yap 1997).

When inserted in the oral environment, restorative materials are exposed to saliva, pH changes and other factors such as food and liquid. To be able to know how the hardness of HA–silica nanocomposite-added GIC is affected by different oral phenomena, further investigation is required. Both *in vivo* and *in vitro* biological characterizations needs to be carried out to determine the biocompatibility of this new material. The results from these further studies also provide a crucial thorough overview and better understanding of the mechanical properties of HA–silica nanocomposite-added GIC for which it might be a promising restorative material.

4. Conclusions

TEM and SEM characterizations revealed that the morphology of HA–silica nanocomposite was a mixture of spherical silica particles embedded within elongated HA. The addition of HA–silica nanocomposite enhances the hardness of pure GIC. The Vickers hardness of HA–35SiO_2–GIC is higher than that of HA–21SiO_2–GIC, HA–11SiO_2–GIC, with the highest hardness achieved by 5% HA–35SiO_2–GIC (70·8HV $\pm$ 11·20) giving $\sim$73% improvement. It can be concluded that addition of HA–silica nanopowder resulted in denser cement and produced a stronger GIC. Application of HA–silica–GIC with improved hardness property might lead to extended clinical indications, especially in stress bearing areas.

Acknowledgements

Financial support of this research work is given by Malaysian Ministry of Higher Education under fundamental Research Grant Scheme (FRGS/203/PPSG/6171138) is highly acknowledged. Authors also thank Ms Quah Su Yin for doing part of the work.

References

Arcis R W, López-Macipe A, Toledano M, Osorio E, Rodríguez-Clemente R, Murtra J, Fanovich M A and Pascual C D 2002 *J. Dent. Mater.* **18** 49

Arita K, Lucas M E and Nishino M 2003 *J. Dent. Mater.* **22** 126

Dorozhkin S V 2010 *Acta Biomater.* **6** 715

Green D L, Lin J S, Lam Y F, Hu M Z C, Schaefer D W and Harris M T 2003 *J. Colloid Interface Sci.* **266** 346

Gu Y W, Yap A U J, Chang P and Khor K A 2005 *Biomaterials* **26** 713

Jafarzadeh M, Rahman I A and Sipaut C S 2009 *J. Sol–Gel Sci. Technol.* **50** 328

Kawata M, Uchida H, Itatani K, Okada I, Koda S and Aizawa M 2004 *J. Mater. Sci. Mater. Med.* **15** 817

Kerby R E and Bleiholder R F 1991 *J. Dent. Res.* **70** 1385

Lohbauer U, Frankenberger R, Clare A, Petschelt A and Greil P 2004 *Biomaterials* **25** 5217

Lohbauer U 2010 *Materials* **3** 76

Lucas M E, Arita K and Nishino M 2003 *Biomaterials* **24** 3787

Magni E, Ferrari M, Hickel R and Ilie N 2010 *Clin. Oral Investig.* **14** 79

McLean J W and Gasser O 1985 *Quint. Int.* **16** 333

Miyaji F, Kono Y and Suyama Y 2005 *Mater. Res. Bull.* **40** 209

Moshaverinia A, Ansari S, Moshaverinia M, Roohpour N, Darr J A and Rehman I 2008 *Acta Biomater.* **4** 432

Nicholson J W, Hawkins S J and Smith J E 1993 *J. Mater. Sci: Mater. Med.* **4** 418

Panda R N, Hsieh M F, Chung R J and Chin T S 2003 *J. Phys. Chem. Solids* **64** 193

Rahman I A, Vejaykumaran P, Sipaut C S, Ismail J, Abu Bakar M, Adnan R and Chee C K 2007 *Colloid Surface A* **294** 102

Rehman I and Bonfield W 1997 *J. Mater. Sci. Mater. Med.* **8** 1

Rozita A R, Rohana A, Mohamad A B and Sam'an M M 2011 *J. Phys. Sci.* **22** 25

Shintome L K, Nagayassu M P, Nicoló R D and Myaki S I 2009 *Brazilian Oral Res.* **23** 439

Silva R C, Zuanon A C C, Candido M S M and Machado J S 2007 *J. Mater. Sci: Mater. Med.* **18** 139

Varma H K and Babu S S 2005 *Ceram. Int.* **31** 109

Vasant E F, Van Der Voort P and Vranchen K C 1995 *Characterization and chemical modification of the Silica surfaces* (New York: Elesvier Sciences)

Walls A W G 1986 *J. Dent.* **14** 231

Wang J and Shaw L L 2009 *Biomaterials* **30** 6565

Xie D, Brantley W A, Culbertson B M and Wang G 2000 *Dent. Mater.* **16** 129

Yap A U J 1997 *J. Mater. Sci: Mater. Med.* **8** 413

Yap A U J, Pek Y S, Kumar R A, Cheang P and Khor K A 2002 *Biomaterials* **23** 955

Yli-Urpo H, Lassila L V J, Nrähi T and Vallittu P K 2005 *J. Dent. Mater.* **21** 201